 CMC, vol.22, no.3, pp.239-260, 2011

Estimation of Natural-Convection Heat-Transfer Characteristics from Vertical Fins Mounted on a Vertical Plate

H. T. Chen[1], K. H. Hsu[1], S. K. Lee[1] and L. Y. Haung[1]

Abstract: The inverse scheme of the finite difference method in conjunction with the least-squares scheme and experimental measured temperatures is proposed to solve a two-dimensional steady-state inverse heat conduction problem in order to estimate the natural-convection heat transfer coefficient under the isothermal situation $\overline{h}^{iso}$ from three vertical fins mounted on a vertical plate and fin efficiency η_f for various values of the fin spacing and fin height. The measured fin temperatures and ambient air temperature are measured from the present experimental apparatus conducted in a small wind tunnel. The heat transfer coefficient on the middle fin of three vertical fins is non-uniform for the present problem and its functional form can be difficult to be obtained. Thus the whole fin is divided into several sub-fin regions before performing the inverse calculation. In order to validate the reliability of the present estimates, the present estimates of $\overline{h}^{iso}$ compare with those obtained from the correlations recommended by current textbooks and other previous results. The present estimates of $\overline{h}^{iso}$ can be applied to obtain a modified correlation of the Nusselt number and Raleigh number.

Keywords: Hybrid inverse scheme; Heat transfer coefficient; Rectangular fin; Natural convection

1 Introduction

The properly designed fins can be especially attractive for the device of the high-performance heat-sink because they offer a more economical solution to the problem. However, the heat transfer from parallel vertical rectangular fin arrays mounted on the vertical plate or the horizontal plate can exhibit convection, radiation, mutual irradiation between two fins and the complex three-dimensional flow and thermal fields for wider range of fin geometries. It is known that the improvement of the convection and radiation heat transfer rates can result in the decrease of system size

[1] Department of Mechanical Engineering, National Cheng Kung University, Tainan, Taiwan, 701

and weight. Moreover, reliability is also an important concept in engineering design. Thus the estimation of a more accurate heat transfer coefficient from vertical fin arrays mounted on the vertical plate or the horizontal plate is required.

The experimental and numerical studies for heat transfer from parallel rectangular fin arrays mounted on a vertical plate have been studied for a long time [Chen and Chou (2006); Chen and Hsu (2007); Harahap, Lesmana and Dirgayasa (2006); Harahap, Rudianto, and Pradnyana (2005); Rammohan Rao and Venkateshan (1996); Leung, Probert, and Shilston (1985); Leung and Probert (1989a); Leung and Probert (1989b)]. However, most existing studies were empirical in natural. Even though these previous studies provided valuable results for the present problem, findings remained inconclusive especially for comparing experimental results obtained from different correlations. Moreover, these available experimental data can also remain very limited. Thus a more accurate predictive scheme is still needed in order to obtain a new heat transfer correlation based on experimental data. This implies that the estimation of a more accurate heat transfer coefficient on the fin is an important task for the device of the high-performance heat-sink.

The heat transfer from rectangular finned surfaces mounted on a vertical plate for the fin temperature higher than the ambient air temperature has been studied by Harahap, Rudianto and Pradnyana (2005) and Harahap, Lesmana and Dirgayasa (2006). Harahap, Rudianto and Pradnyana (2005) and Harahap, Lesmana and Dirgayasa (2006) respectively applied experimental studies to investigate the effects of miniaturizing the base plate dimensions of horizontally and vertically based straight rectangular fin arrays on the steady-state heat-dissipation performance in natural convection. Rammohan Rao and Venkateshan (1996) employed an experimental technique to investigate the interaction of free convection and radiation in a horizontal four fins array. The fin temperature profile was obtained using the measured temperatures at the fin base and fin tip. Later, they numerically solved one-dimensional fin equation with a convecting-radiating fin array over the data range L = 0.05 m, δ = 0.0015 m, 0.03 m $\leq$ H $\leq$ 0.07 m, 0.01 m $\leq$ S $\leq$0.025 m and k = 205 W/m·K. Leung, Probert, and Shilston (1985), Leung and Probert (1989) and Leung and Probert (1989) systematically investigated the effects of the fin spacing, fin length, fin height and fin thickness on the steady-state thermal performances of rectangular fins protruding from vertical or horizontal rectangular bases under natural convection.

Quantitative studies of the heat transfer processes occurring in the industrial applications require the accurate knowledge of the surface conditions and the thermal physical quantities of the material. It is known that these physical quantities and surface conditions can be predicted using the measured temperature data inside the test material. Such problems are called the inverse heat conduction problems

(IHCP). The inverse heat conduction problems have become an interesting subject recently. The main difficulty of the IHCP is that their estimated result can be very sensitive to changes in the measured temperature data resulting from measurement errors [Özisik (1993); Kurpisz and Nowak (1995)]. To date, various inverse methods have been developed for the analysis of the IHCP, such as the implicit finite-difference, regularization, conjugate gradient, function specification, Kalman filter, group preserving, Lie-group and hybrid methods [Hensel (1991); Özisik (1993); Kurpisz and Nowak (1995); Chang, Liu, and Chang (2005); Liu (2008a, 2008b)].

The finite difference method in conjunction with the least-squares scheme and experimental measured temperatures have been applied to estimate the heat transfer coefficient on the vertical plate fin and vertical annular circular fin of one-tube plate finned-tube heat exchangers and fin efficiency for various values of the fin spacing in natural convection by Chen and Chou (2006) and Chen and Hsu (2007). Later, Chen, Liu and Lee (2010) applied the above inverse method in conjunction with experimental measured temperatures to predict the natural-convection heat transfer coefficient under the isothermal situation $\overline{h}^{iso}$ and fin efficiency η_f from a three fin array mounted on a horizontal plate for various values of the fin spacing and fin height. The estimated results of $\overline{h}^{iso}$ given by Chen and Chou (2006); Chen and Hsu (2007), and Chen, Liu and Lee (2010) were in good agreement with those obtained from the correlations recommended by current textbooks [Raithby and Hollands (1985); Kreith and Bohn (1993)]. Their estimated results [Chen and Chou (2006); Chen and Hsu (2007); Chen, Liu and Lee (2010)] also showed that the natural-convection heat transfer coefficient on the fin was non-uniform. This implies that the conventional analysis assuming the uniform heat transfer coefficient on the fin may be inadequate. Chen and Wang (2008) applied the finite difference method in conjunction with experimental measured temperatures given by Lin, Hsu, Chang and Wang (2001) and least-squares method to predict the average overall heat transfer coefficient and wet fin efficiency under wet conditions on vertical square fin arrays mounted on a horizontal plate for various values of the air speed and relative humidity. It can be found that the estimates of the average overall heat transfer coefficient on a fin $\overline{h}$ obtained from the one-dimensional (1-D) and two-dimensional (2-D) models agree well with the exact values even for the simulated temperature measurements with measurement errors [Chen and Wang (2008)]. However, the estimates of the $\overline{h}$ value and the wet fin efficiency obtained from the 2-D model can slightly deviate from those obtained from the 1-D model. It was known that the measurements of the local heat transfer coefficient on a fin under steady-state conditions may be very difficult to be performed, since the local fin temperature and local heat flux must be required. Under the circumstance, the fin efficiency was often determined under the assumption of the uniform heat transfer coefficient. Thus,

the present study further applies the similar inverse scheme proposed by Chen, Liu and Lee (2010) in conjunction with experimental temperature data measured from the present experimental apparatus conducted in a small wind tunnel to predict the values of $\overline{h}^{iso}$ and η_f from three vertical fins mounted on a vertical plate for various values of the fin height and fin spacing. In order to validate the reliability and accuracy of the present estimates, a comparison of the $\overline{h}^{iso}$ values between the present estimates and those obtained from the previous correlations recommended by the current textbook [Raithby and Hollands (1985); Leung and Probert (1989a); Harahap, Lesmana and Dirgayasa (2006)] will be made for various values of the fin spacing and fin height.

2 Mathematical formulation

A 2-D inverse heat conduction problem is introduced to estimate the unknown heat transfer coefficient from three vertical fins mounted on a vertical plate and fin efficiency for various values of the fin spacing and fin height. The experimental temperature data of the fin and ambient air temperature are measured from the experimental apparatus conducted in a small wind tunnel, as shown in Fig. 1. Fig. 2 shows the physical geometry of the 2-D thin fin with measurement locations and sub-fin regions, where L, H and r_o denote the length, height and thickness of the rectangular fin, respectively. Due to the thin fin behavior, the temperature gradient in the Z-direction (the fin thickness) is small and the fin temperature varies only in the X and Y directions. The "insulated tip" assumption can be an adequate approximation provided that the actual heat transfer rate dissipated through the tip is much smaller than the total heat transfer rate drawn from the base wall. The heat transfer coefficient on a fin can be estimated provided that the fin temperatures at various measurement locations and ambient air temperature can be measured. For the direct heat conduction problems, the temperature field can be determined provided that h(X, Y) is given. However, h(X, Y) is unknown for the inverse heat conduction problems (IHCP). It cannot be estimated unless additional information of the measured fin temperatures can be given. The estimated results of Chen and Chou (2006), Chen and Hsu (2007), and Chen, Liu and Lee (2010) showed that the heat transfer coefficient on a fin was non-uniform. Thus, the heat transfer coefficient h(X, Y) in the present study is also assumed to be non-uniform. The thermocouples are fixed at some specific measurement locations of the sub-fin regions in order to record the fin temperatures. The IHCP investigated here involve the estimates of the unknown heat transfer coefficient and fin efficiency. Under the assumptions of the steady state and constant thermal properties, the 2-D heat conduction equation

for the continuous thin fin can be expressed as

$$\frac{\partial^2 T}{\partial X^2} + \frac{\partial^2 T}{\partial Y^2} \frac{2h(X-Y)}{k_f \delta}(T - T_\infty) \text{ for } 0 < X < H,\ 0 < Y < L \tag{1}$$

Its corresponding boundary conditions are

$$T(0,Y) = T_0 \tag{2}$$

$$\frac{\partial T}{\partial X} = 0 \text{ at } X = H \tag{3}$$

and

$$\frac{\partial T}{\partial Y} = 0 \text{ at } Y = 0 \text{ and } Y = L \tag{4}$$

where T is the fin temperature. X and Y are Cartesian coordinates. Δy is the thermal conductivity of the fin. h(X, Y) is the unknown heat transfer coefficient on the fin and is the combination of the convection and radiation heat transfer coefficients because of the fin surface temperature higher than the ambient air temperature. T_o and T_∞ respectively denote the average fin base temperature and ambient air temperature.

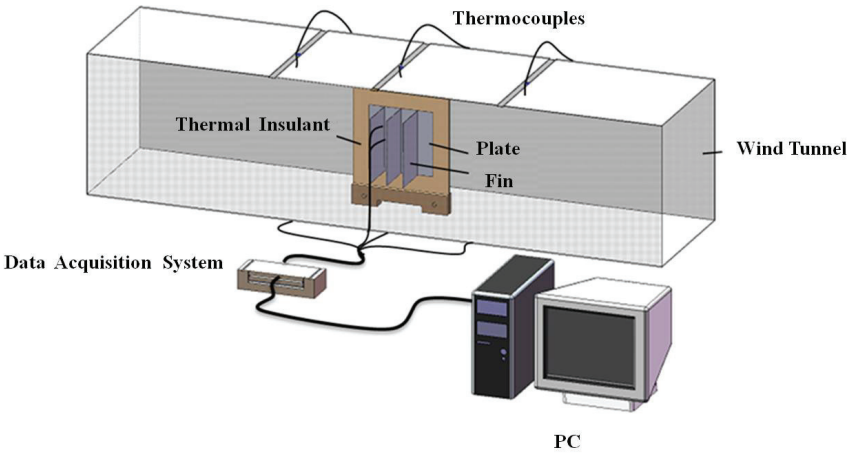

Figure 1: Experimental apparatus configuration of the present study conducted in a small wind tunnel.

3 Numerical analysis

In order to apply the measured fin temperatures and ambient air temperature to predict the unknown average heat transfer coefficient and fin efficiency for various values of the fin height and fin spacing, the vertical rectangular fin is divided into N sub-fin regions and then the unknown heat transfer coefficients on each sub-fin region can be approximated by a constant value. Thus, the application of the finite difference method to Eq. (1) can produce the following difference equation on the *k*th sub-fin region as

$$\frac{T_{i+1,j}-2T_{i,j}+T_{i-1,j}}{\ell_x^2}+\frac{T_{i,j+1}-2T_{i,j}+T_{i,j-1}}{\ell_y^2}=\frac{2\bar{h}_k}{f_k\delta}T_{i,j} \tag{5}$$

for i = 1, 2,. . . , N_y, j = 1, 2,. . . ,N_x and k = 1, 2,. . . , N.

where N_x and N_y are the nodal numbers in X- and Y-directions, respectively. ℓ_x and ℓ_y respectively are the distance between two neighboring nodes in the X- and Y-directions and are defined as $\ell_x = H/(N_x-1)$ and $\ell_y = L/(N_y-1)$. $\bar{h}_k$ denotes the average heat transfer coefficient on the *k*th sub-fin region. N denotes the number of the sub-fin regions

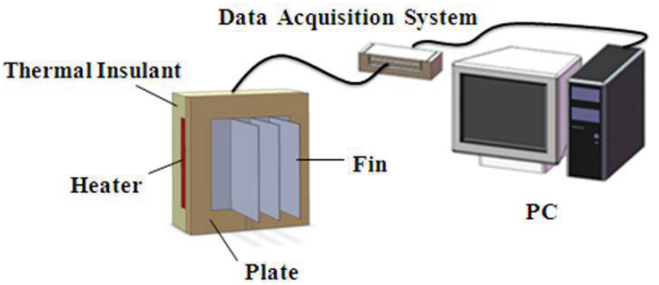

Figure 2: Physical geometry of the present problem with measurement locations and sub-fin regions.

The finite difference forms of the boundary conditions (2)-(4) can be written as

$$T_{i,0}=T_{i,2} \text{ and } T_{i,N_y-1}=T_{i,N_y+1} \text{ for } i=1,2,\ldots,N_x \tag{6}$$

$$T_{1,j}=T_0 \text{ and } T_{N_x-1,j}=T_{N_x+1,j} \text{ for } j=1,2,\ldots,N_y \tag{7}$$

Substitution of Eqs. (6) and (7) into their corresponding difference equations can obtain the difference equations at the boundary surfaces as

$$\frac{T_{i-1,1}-2T_{i,1}+T_{i+1,1}}{(\ell_x)^2}+\frac{2T_{i,2}-2T_{i,1}}{(\ell_y)^2}=\frac{2\bar{h}_k}{k_f\delta}T_{i,1} \text{ for } k=1,N/2+1 \tag{8}$$

$$\frac{T_{i-1,N_y}-2T_{i,N_y}+T_{i+1,N_y}}{(\ell_x)^2}+\frac{2T_{i,N_y-1}-2T_{i,N_y}}{(\ell_y)^2}=\frac{2\bar{h}_k}{k_f\delta}T_{i,N_y} \text{ for } k=N/2,N \tag{9}$$

and

$$\frac{T_{i+1,N_y}-2T_{i,N_y}+T_{i-1,N_y}}{(\ell_x)^2}+\frac{2T_{i,N_y-1}-2T_{i,N_y}}{(\ell_y)^2}=\frac{2\bar{h}_k}{k_f\delta}T_{i,N_y} \text{ for } k=N/2+1,\ldots,N \tag{10}$$

The difference equations for the nodes at the interface between two neighboring sub-fin regions, are given as

$$\frac{2T_{i-1,N_y}-2T_{i,N_y}}{\ell_x^2}+\frac{T_{i,N_y-1}-2T_{i,N_y}+T_{i,N_y+1}}{\ell_y^2}=\frac{2\bar{h}_k}{k_f\delta}T_{i,N_y}$$
$$\text{for } k=1,\ldots,N/2+1 \text{ and } N/2+1,\ldots,N+1 \tag{11}$$

The difference equations for the nodes between four neighboring sub-fin regions are given as

$$\frac{T_{i+1,j}-2T_{i,j}+T_{i-1.j}}{\ell_x^2}+\frac{T_{i,j+1}-2T_{i,j}+T_{i,j-1}}{\ell_y^2}=\frac{\bar{h}_k+\bar{h}_{k+1}+\bar{h}_{k+N/2}+\bar{h}_{k+1+N/2}}{2k_f\delta}T_{i,j}$$
$$\text{for } k=1,2,\ldots,N/2-1 \tag{12}$$

Rearrangement of Eqs. (5), (6), and (8)-(12) can yield the following matrix equation as

$$[K][T]=[F] \tag{13}$$

where [K] is a global conduction matrix. [T] is a matrix representing the nodal temperatures. [F] is a force matrix. The fin temperatures at specific measurement locations can be obtained from Eq. (13) using the Gauss elimination algorithm.

Due to the assumption of the constant heat transfer coefficient on each sub-fin region, the heat transfer rate dissipated from this sub-fin region q_i is

$$q_i=2\bar{h}_j\int_{A_j}(T-T_\infty)dA \text{ for } j=1,2,\ldots,N \tag{14}$$

The average heat transfer coefficient on the fin $\bar{h}$ can be expressed as

$$\bar{h} = \sum_{j=1}^{N} \bar{h}_j A_j / A_f \tag{15}$$

where A_f is the lateral surface area of the fin.

The actual total heat transfer rate dissipated from the rectangular fin to the ambient Q can be written as

$$Q = \sum_{j=1}^{N} q_j = 2A_f (T_0 - T_\infty) \bar{h}^{iso} \tag{16}$$

where $\bar{h}^{iso}$ denotes the heat transfer coefficient on the fin under the isothermal situation.

The fin efficiency η_f is defined as the ratio of the actual total heat transfer rate dissipated from the fin to the heat dissipated from the fin maintained at the average fin base temperature T_o and is expressed as

$$\eta_f = \frac{\sum_{j=1}^{N} q_j}{2A_f (T_0 - T_\infty) \bar{h}} = \frac{\bar{h}^{iso}}{\bar{h}} \tag{17}$$

In order to estimate the unknown heat transfer coefficient $\bar{h}_j$ on the jth sub-fin region, additional information of measured fin temperatures is required at N interior selected measurement locations, as shown in Fig. 2. The measured fin temperature taken from the jth thermocouple is denoted by T_j^{mea} , j = 1,..., N, as shown in Tables 1-4.

The least-squares minimization technique is applied to minimize the sum of the squares of the deviations between the calculated and measured fin temperatures at selected measurement locations. The error in the estimates $E(\bar{h}_1, \bar{h}_2, ..., \bar{h}_N)$ is defined as

$$E(\bar{h}_1, \bar{h}_2, ..., \bar{h}_N) = \sum_{j=1}^{N} \left[T_j^{cal} - T_j^{mea} \right]^2 \tag{18}$$

where the calculated fin temperature at the jth thermocouple location, T_j^{cal}, is determined from Eq. (13).

The estimated values of $\bar{h}_j$, j = 1, 2,..., N, are determined until the value of $E(\bar{h}_1, \bar{h}_2, ..., \bar{h}_N)$ is minimum. The detailedly computational procedures for estimating the unknown value $\bar{h}_j$ can be found from the work of Chen, Liu and Lee (2010).

In order to avoid repetition, they are not shown in this manuscript. The computational procedures of the present study are repeated until the values of $\left|\frac{T_j^{mea}-T_j^{cal}}{T_j^{mea}}\right|$ for j = 1, 2,..., N are all less than 10^{-5}. Once the $\bar{h}_j$ values, j = 1, 2,..., N, are determined, the average heat transfer coefficient $\bar{h}$, heat transfer coefficient under the isothermal situation $\bar{h}^{iso}$, total heat transfer rate Q and fin efficiency η_f can be obtained from Eqs. (15)-(17).

4 Experimental apparatus

An experimental configuration of the small wind tunnel with 3.2 m in length, 0.22 m in width and 0.22 m in height used for the present problem is shown in Fig. 1. This wind tunnel is made of acrylic-plastic sheets with 2 mm in thickness. Its left and right surfaces of this wind tunnel are open. It can be observed from Fig. 1 that the array of three vertical rectangular fins with 0.1 m in length and 0.001 m in thickness are vertically mounted on the outer surface of the vertical plate with 0.1 m in length, 0.1 m in width and 0.006 m in thickness. In order to heat three parallel rectangular fins, a square heater with 0.08 m in length is fixed on another surface of this plate using the adhesive tapes (Nitto Denko Co., Ltd). Later, the test fins and vertical plate enclosed the insulated material are placed in a small wind tunnel and then is heated about 7600 seconds using the 40W heater. Fig. 3 shows the schematic diagram of three parallel rectangular fins vertically mounted on a vertical plate in natural convection. The test fins and vertical plate are made of AISI 304 stainless material. It can be found from Arpaci, Kao and Selamet (1999) that the thermal conductivity of AISI 304 stainless material is 14.9 W/m·K. Its emissivity ε measured by using FT-IR Spectrum 100 (Perkin Elmer Co., Ltd) is 0.18. The ambient air temperature and test fin temperature are measured using T-type thermocouples. The limit of error of the T-type thermocouple is $\pm 0.4\%$ for $0\ ^oC \leq$ T $\leq 350\ ^oC$. Four thermocouples placed in the gap between the fin and the vertical plate are fixed at (0, L/8), (0, 3L/8), (0, 5L/8) and (0, 7L/8) in order to obtain the fin base temperature T_0. Their gap is filled with the cyanoacrylate (Satlon, D-3) in order to reduce the heat loss between the fin and the vertical plate. The thermal contact resistance between the fin and the vertical plate can be neglected in the present study. Experimental temperature data show that these four measured temperatures may have a slight deviation. However, in order to make a comparison of the $\bar{h}^{iso}$ values between the present estimates and those obtained from the correlations recommended by current textbooks [Raithby and Hollands (1985)] and the previous results [Harahap, Lesmanaand and Dirgayasa (2006)]. Thus, the average of these four measured temperatures is taken as the fin base temperature T_0. In order to measure the ambient air temperature T_∞, two thermocouples penetrated the

central line of two lateral surfaces are positioned at 25 mm away from the test fin. One thermocouple is positioned at the top surface, as shown in Fig.1. The average of these three measured temperatures is taken as the ambient air temperature T_∞. Chen, Liu and Lee (2010) applied the present inverse method in conjunction with experimental measured temperatures to predict the natural-convection heat transfer coefficient under the isothermal situation $\overline{h}^{iso}$ and fin efficiency η_f from a three fin array mounted on a horizontal plate for various values of the fin spacing and fin height. Their estimated results of $\overline{h}^{iso}$ [Chen, Liu and Lee (2010)] agreed well with those obtained from the correlations recommended by current textbooks [Raithby and Hollands (1985); Kreith and Bohn (1993)]. This implies that the present inverse method can also give a good accuracy of the present estimates for various values of the fin height and fin spacing. In order to obtain the present estimates, the vertical rectangular fin is divided into eight regions in the present study, i.e., N = 8. These eight thermocouples are respectively fixed at (H/4, L/8), (3H/4, L/8), (H/4, 3L/8), (3H/4, 3L/8), (H/4, 5L/8), (3H/4, 5L/8), (H/4, 7L/8) and (3H/4, 7L/8), as shown in Fig. 2.

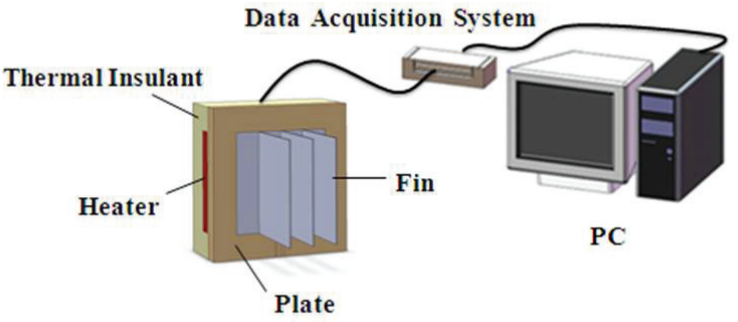

Figure 3: Schematic diagram of three parallel rectangular fins vertically mounted on a vertical plate

5 Results and discussion

The ratio of the surface area of the fin tip to the total fin surface area can be written as $\frac{(2H+L)\delta}{2LH+(2H+L)\delta}$. The "insulated tip" assumption in the present study will be reasonable provided that this ratio is very small. For simplicity, the average heat-transfer coefficient on the tip surface can be assumed to be the same as that on the lateral

surfaces of the fin. Under the condition of L = 0.1 m and δ = 0.001 m, the ratio of the surface area of the fin tip to the total fin surface area, $\frac{(2H+L)\delta}{2LH+(2H+L)\delta}$, is about 1.6% for H = 0.08 m and 2.2% for H = 0.04 m. This implies that the assumptions of Eqs. (2) and (4) should be reasonable for the present study.

Table 1: Comparison of the $\bar{h}_j$ and $\bar{h}$ values between the present estimates and exact results for h(x, y) = $50(XY)^{1/4}$, H = 0.04 m and various ω values.

	T_j^{mea}(K)	Present estimates		Exact results	
		$\bar{h}_j$ (W/m^2K)	$\bar{h}$ (W/m^2K)	$\bar{h}_j$ (W/m^2K)	$\bar{h}$ (W/m^2K)
$\omega = 0\%$	$T_1^{mea} = 340.00$	$\bar{h}_1 = 4.37$	7.84	$\bar{h}_1 = 4.22$	7.74
	$T_2^{mea} = 338.61$	$\bar{h}_2 = 6.35$		$\bar{h}_2 = 6.14$	
	$T_3^{mea} = 337.65$	$\bar{h}_3 = 7.13$		$\bar{h}_3 = 7.00$	
	$T_4^{mea} = 337.08$	$\bar{h}_4 = 7.80$		$\bar{h}_4 = 7.62$	
	$T_5^{mea} = 328.51$	$\bar{h}_5 = 6.12$		$\bar{h}_5 = 6.23$	
	$T_6^{mea} = 326.05$	$\bar{h}_6 = 9.29$		$\bar{h}_6 = 9.08$	
	$T_7^{mea} = 324.24$	$\bar{h}_7 = 10.31$		$\bar{h}_7 = 10.34$	
	$T_8^{mea} = 323.21$	$\bar{h}_8 = 11.32$		$\bar{h}_8 = 11.26$	
$\omega = 0.4\%$	$T_1^{mea} = 340.11$	$\bar{h}_1 = 3.89$	7.87		
	$T_2^{mea} = 338.41$	$\bar{h}_2 = 7.58$			
	$T_3^{mea} = 337.80$	$\bar{h}_3 = 6.14$			
	$T_4^{mea} = 336.96$	$\bar{h}_4 = 8.58$			
	$T_5^{mea} = 328.54$	$\bar{h}_5 = 6.21$			
	$T_6^{mea} = 326.16$	$\bar{h}_6 = 8.85$			
	$T_7^{mea} = 324.17$	$\bar{h}_7 = 10.76$			
	$T_8^{mea} = 323.32$	$\bar{h}_8 = 11.94$			

In practical applications, the actual measured temperature profile often exhibits random oscillations due to measurement errors. On the other hand, due to experimental uncertainties, most realistic measurements should add simulated small random errors to the direct solution obtained from the related direct problem. Thus, in order to simulate the experimental measured temperature T_j^{mea}, the direct solution T_j^{exa} should be modified by adding small random error. The simulated experimental temperatures can be expressed as

$$T_j^{\exp} = T_j^{exa}(1 \pm \omega) \text{ for } j = 1, 2, \ldots, N \tag{19}$$

where ω is a random number generated by the subroutine QuickBASIC 4.50 and is assumed to be within 5% in the present study.

In order to validate the accuracy and reliability of the present inverse scheme, an example with h(x, y) = $50(XY)^{1/4}$ is illustrated. Later, the direct solution T_j^{exa} at selected measurement locations can be determined using the present numerical method. Table 1 shows comparison of the $\overline{h}_j$ and $\overline{h}$ values between the present estimates and exact results for h(x, y) = $50(XY)^{1/4}$, T_0 = 350 K, T_∞ = 300 K, H = 0.04 m, N = 8, N_x = 41, N_y = 17 and various ω values. It can be found from Table 1 that the present estimates of the average heat transfer coefficient $\overline{h}$ agree well with the exact results for the limit of error of the thermocouple ω = 0 % and 5%. The maximum error of the $\overline{h}$ value is about 1.7% for ω = 5%. The present estimates of the average heat transfer coefficient on the jth sub-fin region $\overline{h}_j$, j = 1, 2,. . . , 8, are also in good agreement with the exact results for ω = 0%. However, the present estimates of the $\overline{h}_j$ values slightly deviate from the exact values for ω = 5%.

All the physical properties are evaluated at the film temperature or the average of the fin base temperature and ambient air temperature for the present problem. All the computations are performed with N = 8, N_x = 41 and N_y = 17. The unknown heat transfer coefficients $\bar{h}_j$ for j = 1, 2,. . . , N used to begin the iterations are taken as unity. The measured temperatures, T^{mea}(H/4, L/8), T^{mea} (3H/4, L/8), T^{mea} (H/4, 3L/8), T^{mea} (3H/4, 3L/8), T^{mea} (H/4, 5L/8), T^{mea} (3H/4, 5L/8), T^{mea} (H/4, 7L/8) and T^{mea} (3H/4, 7L/8) are respectively denoted as T_1^{mea}, T_2^{mea}, T_3^{mea}, T_4^{mea}, T_5^{mea}, T_6^{mea}, T_7^{mea} and T_8^{mea}. The thermal boundary layer starts to develop at the bottom of the test fin and increases in thickness along the fin for the present problem. Moreover, the test fin is also heated at X = 0. Thus, it can be found from Tables 2-4 that the measured fin temperatures at the measurement locations (H/4, Y) are not equal to those at the measurement locations (3H/4, Y) for 0.02 m $\geq$ S $\geq$ 0.005 m and 0.08 m $\geq$ H $\geq$ 0.04 m. In addition, the fin temperature T_4^{mea} can nearly be the highest temperature, and the fin temperatures at the measurement locations on the top fin region are higher than those on the bottom fin region. It is also observed an interesting results from Tables 2-4 that there is a considerable temperature drop from the fin base (X = 0) to X = H/4 for 0.02 m $\geq$ S $\geq$ 0.005 m and 0.08 m $\geq$ H $\geq$ 0.04 m. The fin temperature increases from Y = 0 to Y = L at the same X value. However, the measured fin temperatures at the measurement locations (X, 5L/8) are nearly equal to those at (X, 7L/8). Due to the poor thermal conductivity of the stainless fin, there is a considerable temperature drop from the fin base to the edge of the fin. The fin temperature distributions obviously depart from the ideal isothermal situation.

Tables 2-5 respectively show the effect of the fin spacing S on the average heat transfer coefficient on the jth sub-fin region $\overline{h}_j$, total heat transfer rate from the whole fin Q, average heat transfer coefficient $\overline{h}$, heat transfer coefficient under the isotherm condition $\overline{h}^{iso}$ and fin efficiency η_f for 0.04 m $\leq$ H $\leq$ 0.08 m. Tables

2-5 also show that the average heat transfer coefficient on the jth sub-fin region $\overline{h}_j$ deviates from $\overline{h}_{j+4}$ for j = 1, 2, 3 and 4. This phenomenon may result from that a complex three-dimensional flow and thermal fields or the formation of irregular chimney flow patterns within two vertical rectangular fins may occur for the present problem.

The average heat transfer coefficient on each sub-fin region can be sensitive to the measured fin temperatures. Tables 2-5 show that the average heat transfer coefficient on each sub-fin region can be the random distribution for S $\geq$ 0.005 m and 0.04 m $\leq$ H $\leq$ 0.08 m. At the same time, an interesting result that the average heat transfer coefficient on the sub-fin region 1, $\overline{h_1}$, can be higher than those on other sub-fin regions for S $\geq$ 0.005 m and 0.04 m $\leq$ H $\leq$ 0.08 m.

Various heat transfer correlations for the present problem have been proposed [Harahap, Lesmana and Dirgayasa (2006); Leung and Probert (1989a); Leung and Probert (1989b); and Raithby and Hollands (1985); Harahap and Setio (2001)]. However, among these heat transfer correlations, the correlations given by Harahap, Lesmana and Dirgayasa (2006), Leung and Probert (1989a) and Raithby and Hollands (1985) are selected to compare with the present estimated results. It can be found from Raithby and Hollands (1985) that Van De Pol and Tierney (1973) proposed the following correlated relationship between Nu_r and Ra_r to fit the data of Welling and Wooldridge (1965) in the range $0.6 < Ra_r < 100$, Pr = 0.71, 0.33 < L/S < 4.0 and 4.2 < H/S < 10.6 as

$$Nu_r = \frac{Ra_r}{\psi}\left\{1-\exp[-\psi(\frac{0.5}{Ra_r})^{3/4}]\right\} \tag{20}$$

where the Prandtl number Pr is defined as $\mathrm{Pr} = \nu/\alpha$. Nu_r and Ra_r are defined as $Nu_r = \bar{h}^{iso} r/k_{air}$ and $Ra_r = g\beta(T_o - T_\infty)r^3/(\nu\alpha_{air})$. g is the acceleration of gravity. β is the volumetric thermal expansion coefficient. k_{air}, ν and α_{air} are the thermal conductivity, kinematic viscosity and thermal diffusivity of the air, respectively. The parameter r denotes r =2LS/(2L+S). The parameter ψ is defined as

$$\psi = \frac{24(1-0.483e^{-0.17L/S})}{\{(1+0.5S/L)[1+(1-e^{-0.83S/L})(9.14e^{-4.65S}\sqrt{S/L}-0.61]\}} \tag{21}$$

Harahap, Lesmana and Dirgayasa (2006) also proposed a correlation of Nu, Ra, S/L, W/L and S/H for the vertically based array, H = 0.0135 m, 0.003 m $\leq$ S $\leq$ 0.011 m, 0.025 m $\leq$ L $\leq$ 0.049 m, δ = 0.001 m and $2\times10^5 \leq (L/S)^3 Ra \leq 5\times10^5$ as

$$Nu = 3.35Ra^{0.153}(S/L)^{0.541}(L/W)^{0.121}(S/H)^{0.605} \tag{22}$$

where Nu and Ra are defined as $Nu = \bar{h}^{iso} S/k_{air}$ and $Ra = g\beta(T_o - T_\infty)S^3/(\nu\alpha_{air})$. The parameter W denotes the width of the fin arrays and is defined as W = 3δ + 2S in the present study. Obviously, Eq. (22) was valid in the range 0.06 < S/L < 0.44 and 0.27 < H/L < 0.54.

Harahap, Lesmana and Dirgayasa (2006) stated that Leung and Probert (1989a) applied non-dimensional parameters in conjunction with their sets of more than 300 experimental data to obtain the following correlations as

$$Nu = 0.135 Ra^{*0.5} \text{ for } Ra^* \leq 250 \tag{23}$$

and

$$Nu = 0.423 Ra^{*1/3} \text{ for } 250 < Ra^* < 10^6 \tag{24}$$

where the modified Rayleigh number Ra* is defined as $Ra^* = Ra \exp(-\frac{k_{air}H}{k\delta})(\frac{S^2}{LH})^{0.5}$. Leung and Probert (1989b) performed additional experiments using highly polished duralumin fin arrays with small fin height for H = 0.01 or 0.017 m, 0.03 m $\leq$ S $\leq$ 0.045 m, L = 0.15 m, W = 0.19 m, δ = 0.003 m and T_f = 20 or 40 K. They obtained the resulting correlations as

$$Nu = 0.144 Ra^{*0.5} \text{ for } Ra^* \leq 250 \tag{25}$$

and

$$Nu = 0.490 Ra^{*1/3} \text{ for } 250 < Ra^* < 10^6 \tag{26}$$

To validate the accuracy and reliability of the present inverse method in conjunction with the present experimental temperature data further, a comparison between the present estimates of the $\bar{h}^{iso}$ value and those obtained from the correlations recommended by Raithby and Hollands (1985), Harahap, Lesmana and Dirgayasa (2006) and Leung and Probert (1989a) is shown in Table 6 for L = 0.1 m and various values of the fin spacing and fin height. Examination of Table 6 shows that the present estimates of the $\bar{h}^{iso}$ value are in good agreement with those obtained from correlation (22) recommended by Harahap, Lesmana and Dirgayasa (2006) for 0.05 $\leq$ S/L $\leq$ 0.2 and 0.6 $\leq$ H/L $\leq$ 0.8. However, the present estimates of the $\bar{h}^{iso}$ value deviate slightly from those obtained from the correlations recommended by Raithby and Hollands (1985), Leung and Probert (1989a) and Harahap, Lesmana and Dirgayasa (2006) for 0.05 $\leq$ S/L $\leq$ 0.2 and H/L = 0.4 m. This deviation may result from measurement errors or the use of the average fin base temperature, etc.

Tables 2-5 also show the present estimates of the total heat transfer rate Q and fin efficiency η_f for various values of the fin spacing and fin height. As shown in Çengel (2004), when the heat sink involves closely spaced fins, the narrow channels

Table 2: Present estimates for H = 0.04 m and various S values.

	S = 0.005 m T_0 = 333.17 K T_∞ = 300.01 K	S = 0.010 m T_0 = 332.26 K T_∞ = 300.83 K	S = 0.015 m T_0 = 328.29 K T_∞ = 298.76 K	S = 0.02m T_0 = 333.56 K T_∞ = 299.95 K
T_j^{mea} (K)	T_1^{mea} =323.27K T_2^{mea} =327.52K T_3^{mea} =329.52K T_4^{mea} =329.71K T_5^{mea} =317.44K T_6^{mea} =322.47K T_7^{mea} =325.49K T_8^{mea} =326.38K	T_1^{mea} =319.69K T_2^{mea} =320.83K T_3^{mea} =325.73K T_4^{mea} =326.51K T_5^{mea} =313.53K T_6^{mea} =316.93K T_7^{mea} =318.95K T_8^{mea} =319.15K	T_1^{mea} =316.09K T_2^{mea} =317.73K T_3^{mea} =321.26K T_4^{mea} =321.47K T_5^{mea} =309.14K T_6^{mea} =311.17K T_7^{mea} =314.65K T_8^{mea} =314.15K	T_1^{mea} =318.20K T_2^{mea} =321.85K T_3^{mea} =321.12K T_4^{mea} =321.28K T_5^{mea} =312.50K T_6^{mea} =314.17K T_7^{mea} =316.02K T_8^{mea} =315.30K
$\overline{h}_j$ (W/m^2K)	$\overline{h_1}$ = 20.17 $\overline{h_2}$ = 4.69 $\overline{h_3}$ = 1.97 $\overline{h_4}$ = 3.22 $\overline{h_5}$ = 8.76 $\overline{h_6}$ = 1.82 $\overline{h_7}$ = 1.87 $\overline{h_8}$ = 1.85	$\overline{h_1}$ = 32.04 $\overline{h_2}$ = 30.94 $\overline{h_3}$ = 3.59 $\overline{h_4}$ = 3.48 $\overline{h_5}$ = 5.21 $\overline{h_6}$ = 1.46 $\overline{h_7}$ = 4.73 $\overline{h_8}$ = 8.01	$\overline{h_1}$ = 30.57 $\overline{h_2}$ = 23.97 $\overline{h_3}$ = 6.29 $\overline{h_4}$ = 7.24 $\overline{h_5}$ = 11.28 $\overline{h_6}$ = 9.77 $\overline{h_7}$ = 2.47 $\overline{h_8}$ = 9.90	$\overline{h_1}$ = 33.80 $\overline{h_2}$ = 8.74 $\overline{h_3}$ = 19.96 $\overline{h_4}$ = 16.91 $\overline{h_5}$ = 6.65 $\overline{h_6}$ = 9.17 $\overline{h_7}$ = 1.00 $\overline{h_8}$ = 6.38
Ra	12.36	149.14	592.57	1548.90
$\overline{h}$ (W/m^2K)	5.54	11.18	12.69	12.83
$\overline{h}^{iso}$ (W/m^2K)	4.07	7.18	7.88	8.31
Q (W)	1.08	1.81	1.86	2.23
η_f	0.73	0.64	0.62	0.65

Table 3: Present estimates for H = 0.06 m and various S values.

	S = 0.005 m T_0 = 332.63 K T_∞ = 299.83 K	S = 0.010 m T_0 = 331.37 K T_∞ = 299.81 K	S = 0.015 m T_0 = 328.14 K T_∞ = 299.77 K	S = 0.02m T_0 = 328.56 K T_∞ = 299.13 K
T_j^{mea} (K)	T_1^{mea} =321.02K T_2^{mea} =325.31K T_3^{mea} =326.51K T_4^{mea} =326.92K T_5^{mea} =312.36K T_6^{mea} =316.32K T_7^{mea} =318.07K T_8^{mea} =318.79K	T_1^{mea} =315.39K T_2^{mea} =319.65K T_3^{mea} =321.63K T_4^{mea} =322.14K T_5^{mea} =307.47K T_6^{mea} =309.75K T_7^{mea} =311.06K T_8^{mea} =311.84K	T_1^{mea} =314.67K T_2^{mea} =317.05K T_3^{mea} =318.20K T_4^{mea} =318.03K T_5^{mea} =306.84K T_6^{mea} =307.87K T_7^{mea} =309.70K T_8^{mea} =309.84K	T_1^{mea} =314.92K T_2^{mea} =316.84K T_3^{mea} =315.56K T_4^{mea} =316.13K T_5^{mea} =306.15K T_6^{mea} =307.95K T_7^{mea} =309.07K T_8^{mea} =309.09K
$\overline{h}_j$ (W/m^2K)	$\overline{h_1}$ = 11.67 $\overline{h_2}$ = 0.33 $\overline{h_3}$ = 1.06 $\overline{h_4}$ = 0.85 $\overline{h_5}$ = 9.83 $\overline{h_6}$ = 1.74 $\overline{h_7}$ = 3.70 $\overline{h_8}$ = 3.35	$\overline{h_1}$ = 22.70 $\overline{h_2}$ = 7.99 $\overline{h_3}$ = 4.25 $\overline{h_4}$ = 3.40 $\overline{h_5}$ = 10.73 $\overline{h_6}$ = 4.71 $\overline{h_7}$ = 7.17 $\overline{h_8}$ = 6.40	$\overline{h_1}$ = 18.96 $\overline{h_2}$ = 8.08 $\overline{h_3}$ = 6.54 $\overline{h_4}$ = 8.45 $\overline{h_5}$ = 8.82 $\overline{h_6}$ = 10.18 $\overline{h_7}$ = 3.35 $\overline{h_8}$ = 6.19	$\overline{h_1}$ = 17.09 $\overline{h_2}$ = 7.01 $\overline{h_3}$ = 17.71 $\overline{h_4}$ = 12.98 $\overline{h_5}$ = 12.30 $\overline{h_6}$ = 5.39 $\overline{h_7}$ = 1.93 $\overline{h_8}$ = 4.21
Ra	13.28	176.20	703.31	1996.01
$\overline{h}$ (W/m^2K)	4.06	8.42	8.82	9.83
$\overline{h}^{iso}$ (W/m^2K)	2.35	4.02	4.7	5.08
Q (W)	0.92	1.52	1.60	1.79
η_f	0.58	0.49	0.50	0.52

Table 4: Present estimates for H = 0.08 m and various S values.

	S = 0.005 m T_0 = 331.65K T_∞ = 299.96 K	S = 0.010 m T_0 = 326.38 K T_∞ = 299.72 K	S = 0.015 m T_0 = 326.88 K T_∞ = 299.28 K	S = 0.02m T_0 = 333.56 K T_∞ = 299.95 K
T_j^{mea} (K)	T_1^{mea} =319.72K T_2^{mea} =323.18K T_3^{mea} =323.81K T_4^{mea} =323.52K T_5^{mea} =310.36K T_6^{mea} =311.13K T_7^{mea} =314.51K T_8^{mea} =315.35K	T_1^{mea} =312.06K T_2^{mea} =314.39K T_3^{mea} =315.32K T_4^{mea} =316.01K T_5^{mea} =305.24K T_6^{mea} =306.60K T_7^{mea} =306.64K T_8^{mea} =305.94K	T_1^{mea} =311.18K T_2^{mea} =314.33K T_3^{mea} =315.34K T_4^{mea} =315.48K T_5^{mea} =303.73K T_6^{mea} =305.85K T_7^{mea} =306.95K T_8^{mea} =306.64K	T_1^{mea} =310.18K T_2^{mea} =312.67K T_3^{mea} =314.08K T_4^{mea} =314.89K T_5^{mea} =303.48K T_6^{mea} =304.92K T_7^{mea} =305.35K T_8^{mea} =305.40K
$\overline{h}_j$ (W/m^2K)	$\overline{h_1}$ = 8.19 $\overline{h_2}$ = 0.08 $\overline{h_3}$ = 1.44 $\overline{h_4}$ = 2.46 $\overline{h_5}$ = 7.95 $\overline{h_6}$ = 0.33 $\overline{h_7}$ = 3.65 $\overline{h_8}$ = 1.87	$\overline{h_1}$ = 15.81 $\overline{h_2}$ = 6.16 $\overline{h_3}$ = 6.12 $\overline{h_4}$ = 3.71 $\overline{h_5}$ = 7.81 $\overline{h_6}$ = 0.72 $\overline{h_7}$ = 3.75 $\overline{h_8}$ = 8.94	$\overline{h_1}$ = 18.64 $\overline{h_2}$ = 5.37 $\overline{h_3}$ = 6.00 $\overline{h_4}$ = 6.04 $\overline{h_5}$ = 12.56 $\overline{h_6}$ = 1.85 $\overline{h_7}$ = 1.66 $\overline{h_8}$ = 5.84	$\overline{h_1}$ = 17.78 $\overline{h_2}$ = 10.28 $\overline{h_3}$ = 11.90 $\overline{h_4}$ = 6.83 $\overline{h_5}$ = 6.35 $\overline{h_6}$ = 0.92 $\overline{h_7}$ = 4.19 $\overline{h_8}$ = 5.76
Ra	303.79	2113.06	7380.42	20382.24
$\overline{h}$ (W/m^2K)	3.25	6.63	7.25	8.00
$\overline{h}^{iso}$ (W/m^2K)	1.79	2.88	3.18	3.59
Q (W)	0.91	1.23	1.40	1.93
η_f	0.55	0.43	0.44	0.45

Table 5: Present estimates for a single fin ($S \to \infty$) and various H values.

	H=0.04 m T_0 =331.87 K T_∞ =299.72 K	H=0.06 m T_0 =330.85 K T_∞ =299.50 K	H=0.08 m T_0 =336.24 K T_∞ =299.78 K
T_j^{mea} (K)	T_1^{mea} = 318.59 T_2^{mea} = 319.75 T_3^{mea} = 322.90 T_4^{mea} = 323.41 T_5^{mea} = 311.88 T_6^{mea} = 314.58 T_7^{mea} = 315.78 T_8^{mea} = 315.91	T_1^{mea} = 316.60 T_2^{mea} = 318.12 T_3^{mea} = 317.28 T_4^{mea} = 317.01 T_5^{mea} = 307.31 T_6^{mea} = 308.72 T_7^{mea} = 309.61 T_8^{mea} = 309.77	T_1^{mea} = 315.30 T_2^{mea} = 317.32 T_3^{mea} = 317.92 T_4^{mea} = 319.44 T_5^{mea} = 306.62 T_6^{mea} = 307.84 T_7^{mea} = 307.93 T_8^{mea} = 307.81
$\overline{h}_j$ (W/m^{2}K)	$\overline{h}_1$ = 31.82 $\overline{h}_2$ = 29.73 $\overline{h}_3$ = 11.17 $\overline{h}_4$ = 10.74 $\overline{h}_5$ = 9.70 $\overline{h}_6$ = 1.08 $\overline{h}_7$ = 6.12 $\overline{h}_8$ = 7.94	$\overline{h}_1$ = 15.90 $\overline{h}_2$ = 8.65 $\overline{h}_3$ = 14.99 $\overline{h}_4$ = 15.44 $\overline{h}_5$ = 10.76 $\overline{h}_6$ = 5.86 $\overline{h}_7$ = 3.53 $\overline{h}_8$ = 3.70	$\overline{h}_1$ = 17.78 $\overline{h}_2$ = 10.28 $\overline{h}_3$ = 11.90 $\overline{h}_4$ = 6.83 $\overline{h}_5$ = 6.35 $\overline{h}_6$ = 0.92 $\overline{h}_7$ = 4.19 $\overline{h}_8$ = 5.76
Ra	557779.59	2124934.93	5873994.98
$\overline{h}$ (W/m^{2}K)	13.54	9.85	8.00
$\overline{h}^{iso}$ (W/m^{2}K)	8.38	5.10	3.64
Q (W)	2.16	1.92	2.12
η_f	0.62	0.52	0.45

Table 6: Comparison of $\bar{h}^{iso}$ between the present estimates and previous results for various H and S values.

H (m)	S (m)	$\overline{h}^{iso}$ (W/m^{2}K)			
		Present estimates	Eq. (22)	Eq. (20)	Eqs. (23) and (24)
0.04	0.005	4.07	3.20	3.10	3.57
	0.01	7.18	4.50	5.70	8.21
	0.015	7.88	5.44	6.08	9.24
	0.02	8.31	6.42	6.42	10.57
0.06	0.005	2.35	2.50	2.99	3.16
	0.01	4.02	3.52	5.72	7.60
	0.015	4.70	4.24	6.03	8.42
	0.02	5.08	4.91	6.23	9.37
0.08	0.005	1.79	2.09	2.88	3.16
	0.01	2.88	2.88	5.42	5.26
	0.015	3.18	3.54	6.00	7.86
	0.02	3.59	4.22	6.44	9.19

formed tend to block the fluid, especially when the heat sink is long. As a result, the blocking action produced overwhelms the extra buoyancy and downgrades the heat transfer characteristics of the heat sink. The buoyancy effects dominate when the heat sink involves widely spaced fins. This implies that the heat transfer coefficient under the isotherm condition $\bar{h}^{iso}$ and total heat transfer rate Q increase with increasing the fin spacing for a fixed fin height and with decreasing the fin height for a fixed fin spacing. The η_f value decreases with increasing the fin height. A more variation of the η_f value can occur in the range $0.05 \leq$ S/L ≤ 0.1 for $0.6 \leq$ H/L ≤ 0.8. However, the Q and η_f values can gradually approach an asymptotical value with increasing the fin spacing for a fixed fin height.

6 Conclusions

The present study proposes a numerical inverse scheme involving the finite difference method in conjunction with the least-squares method and experimental measured temperatures to estimate the natural-convection heat transfer coefficient under the isothermal situation $\bar{h}^{iso}$ from vertical fin arrays mounted on a vertical plate, the total heat transfer rate Q and fin efficiency η_f for various values of the fin spacing and fin height. The present estimates of the $\bar{h}^{iso}$ value agree with those obtained from the correlations recommended by the previous works or current textbooks or for $0.05 \leq$ S/L ≤ 0.2 and $0.4 \leq$ H/L ≤ 0.8. This implies that the present inverse method can give a good estimation for various values of the fin height and fin spacing. It is worth noting that that S/L can have a significant effect on the present estimates of $\bar{h}^{iso}$ for S/L ≤ 0.15. In addition, the effect of H/L on the present estimates of $\bar{h}^{iso}$ for $0.4 \leq$ H/L ≤ 0.8 cannot be negligible, too.

References

Arpaci V. S.; Kao S. H.; Selamet A. (1999): *Introduction to Heat Transfer*. Prentice Hall, New Jersey.

Chang C. W.; Liu C. S.; Chang J. R. (2005): A group preserving scheme for inverse heat conduction problems. *CMES: Computer Modeling in Engineering and Sciences*. vol. 10, pp. 13-38.

Çengel Y. A. (2004): *Heat Transfer: A Practical Approach*, second ed., McGraw-Hill Education (Asia), Singapore, pp. 473-477.

Chen H. T.; Chou J. C. (2006): Investigation of natural-convection heat transfer coefficient form the vertical fin of finned-tube heat exchangers. *Int. J. Heat Mass Transfer*, vol. 49, pp.3034-3044.

Chen H. T.; Hsu W. L. (2007): Estimation of heat transfer coefficient on the fin of annular-finned tube heat exchangers in natural convection for various fin spacings. *Int. J. Heat Mass Transfer*. vol. 50, pp. 1750-1761.

Chen, H.T.; Liu, L.S.; Lee, S.K. (2010): Estimation of heat-transfer characteristics from fins mounted on a horizontal plate in natural convection. *CMES: Computer Modeling in Engineering & Sciences*, vol. 1565, pp. 1-21.

Chen H. T.; Wang H. C. (2008): Estimation of heat-transfer characteristics on a rectangular fin under wet conditions. *Int. J. Heat Mass Transfer*, vol. 51, pp. 2123-2138.

Harahap F.; Lesmana H.; Dirgayasa I. K.T. A. S. (2006): Measurements of heat dissipation from miniaturizd vertical rectangular fin arrays under dominant natural convection conditions. *Heat Mass Transfer*, vol. 42, pp.1025-1036.

Harahap F.; Rudianto E.; Pradnyana IGD M. E. (2005): Measurements of steady-state heat dissipation from miniaturizd horizontally-based straight rectangular fin arrays. *Heat Mass Transfer*, vol. 41, pp. 280-288.

Harahap F.; Setio D. (2001): Correlations of heat dissipation and natural convection heat transfer from horizontally based, vertically finned arrays. *Applied Energy*, vol. 69, pp. 29-38.

Hensel E. (1991): *Inverse Theory and Applications for Engineers*, Prentice Hall, Englewood Cliffs, New Jersey.

Jones C. D.; Smith L. F. (1970): Optimum arrangement of rectangular fins on horizontal surfaces for free convection heat transfer. *ASME J. Heat Transfer*, vol. 92, pp. 6-10.

Kreith F.; Bohn M. S. (1993): *Principles of Heat Transfer*, fifth ed., West Publishing Co., New York.

Kurpisz K.; Nowak A. J. (1995): *Inverse Thermal Problems*. Computational Mechanics Publications, Southampton, UK.

Leung C. W.; Probert S. D.; Shilston M. J. (1985): Heat exchanger design: Thermal performances of rectangular fins protruding from vertical or horizontal rectangular bases. *Applied energy*, vol. 20, pp. 123-140.

Leung C. W.; Probert S. D. (1989a): Heat exchanger performance: Effect of orientation. *Applied energy*, vol. 33, pp. 235-252.

Leung C. W.; Probert S. D. (1989b): Thermal effectiveness of short-protrusion rectangular heat exchanger fins. *Applied energy*, vol. 34, pp.1-8.

Lin Y. T.; Hsu K. C.; Chang Y. J.; Wang C. C. (2001): Performance of rectangular fin in wet conditions: Visualization and wet fin efficiency. *ASME J. Heat Transfer*, vol. 123, pp. 827-836.

Liu, C.S. (2008a): An LGEM to identify time-dependent heat conductivity function by an extra measurement of temperature gradient. *CMC: Computers, Materials & Continua*, vol. 7, pp. 81-96.

Liu, C.S. (2008b): The Lie-group shooting method for thermal stress evaluation through an internal temperature measurement. *CMC: Computers, Materials & Continua*, vol. 8, pp. 1-16.

Özisik M. N. (1993): *Heat Conduction (Chapter 14)*. second ed., Wiley, New York.

Raithby G. D.; Hollands K. G. T. (1985): Natural convection, in W. M. Rohsenow, J. P. Hartnett, E. N. Ganic (Eds.), *Handbook of Heat Transfer Fundamentals*, second ed., McGraw-Hill, New York.

Rammohan Rao V.; Venkateshan S. P. (1996): Experimental study of free convection and radiation in horizontal fin arrays. *Int. J. Heat Mass Transfer*, vol. 39, pp. 779-789.

Van De Pol D. W.; **Tierney J. K.** (1973): Free convection Nusselt number for vertical U-shaped channels. *ASME J. Heat Transfer*, vol. 95, pp. 915-926.

Welling J. R.; Wooldridge C.B. (1965): Free convection heat transfer coefficients from rectangular vertical fins. *ASME J. Heat Transfer*, vol. 87, pp. 439-444.